

# PHORETIC FORCE MEASUREMENT FOR MICROPARTICLES UNDER MICROGRAVITY CONDITIONS.

E. J. Davis and R. Zheng, University of Washington, Department of Chemical Engineering, Box 351750, Seattle, WA, 98195-1750, davis@cheme.washington.edu.

## INTRODUCTION

Microparticles can deposit on surfaces under the influence of a variety of forces. In the absence of gravity, forces that would otherwise be negligible become dominant. Even in a gravitational field some of these forces can be much larger than the gravitational force. Among these are the phoretic forces that arise when a small particle exists in a nonuniform gas. In the case of the thermophoretic force, molecules colliding with the particle that come from a higher temperature region exchange more momentum and kinetic energy with the particle than do molecules coming from a lower temperature region. The resulting force can cause the particle to deposit on a colder surface or move away from a higher temperature surface. Applications include particle deposition on semiconductor surfaces and on surfaces in combustion processes, containerless processing, and the production of nanophase materials, pigments and other fine particles.

Momentum and energy transfer associated with gas molecule collisions are not well understood and cannot be predicted from first principles for "engineering" surfaces. Neither of the two limiting cases of perfect accommodation or specular reflection adequately describe most collisions, so in the last century James Clerk Maxwell introduced the concept of accommodation coefficients to describe collisional processes. Experiments are needed to determine accommodation coefficients.

This research program involves theoretical and experimental studies of phoretic forces that act on micrometer-size particles. Phoretic forces are strongly dependent on the mean free path and kinetic energy of the gas molecules, and for a given microparticle monatomic, diatomic and polyatomic gases behave very differently. Li and Davis [1,2] reported measurements using helium, nitrogen and carbon dioxide for a variety of microspheres including nonvolatile liquid droplets, polystyrene latex (PSL) spheres, glass microspheres and metallic nickel spheres. These systems represent a wide range of thermal conductivities and other properties. Li and Davis compared their results with numerous theories in existence, and to make such comparisons it is necessary to know the thermal properties of the gas and microparticle. Furthermore, their work was limited to spherical particles. Many microparticles of interest have irregular shapes and unknown thermal properties, so it is necessary to measure their thermal properties to interpret and predict the thermophoretic force.

To perform thermophoretic force experiments we have built a special electrodynamic balance (EDB)

equipped with heat exchangers mounted in a vacuum chamber. The chamber pressure can be varied to alter the mean free path of the gas molecules. The thermal and radiative properties of microparticles can also be measured by single particle experiments in which a charged microparticle is levitated in an EDB and illuminated with a laser beam. The principles and applications of the EDB have been surveyed by Davis [3,4]. Spjut *et al.* [5] at MIT introduced the electrodynamic thermogravimetric analyzer (EDTGA) for the study of carbonaceous particles, and the MIT group performed a variety of investigations reviewed by Bar-Ziv *et al.* [6]. These include particle temperature measurements by infrared pyrometry and transient heating experiments [7]. Bar-Ziv and Sarofim [8] provided an additional review of the literature associated with particle heating in an EDB, including the effects of microparticle properties on the electromagnetic heat source function.

Monazam *et al.* [9] and Monazam and Maloney [10] at the Morgantown Energy Technology Center (METC) adapted the techniques of Spjut and his co-workers to determine heat capacities, temperatures and absorptivities of single carbon particles by means of pulsed heating experiments. A levitated particle with a diameter of order 100  $\mu\text{m}$  was illuminated from two sides using a CO<sub>2</sub> laser (10.6  $\mu\text{m}$  wavelength) with a repetition rate of 100 Hz and a pulse duration of 3 ms. The particle temperature was determined from measurements of the radiant emissive power of the particle using Planck's distribution law for the monochromatic radiant emission intensity.

The time-dependent temperature distribution in the microsphere was modeled by assuming that the heat flux associated with the electromagnetic radiation is uniform over the surface of the sphere. That is, the heat source was treated as a boundary condition rather than as an electromagnetic heat source within the sphere. Convective and radiative heat losses were included in the surface boundary condition, but for the conditions of the experiments gas phase conduction was the dominant heat loss. They solved the governing unsteady state heat conduction equation numerically, and performed parametric studies, comparing predicted surface temperatures with measured temperatures. The authors recognized that the use of a spatially uniform energy flux at the surface is an approximation that may not be valid for other materials with physical and optical properties that differ from carbon.

It was the objective of part of our recent studies to develop a more rigorous analysis of unsteady state

heating of a sphere by electromagnetic radiation, taking into account a spatially-dependent surface energy flux based on Mie theory. The analysis of the METC group is recovered as a special case of a more general formulation.

## PULSED HEATING OF MICROSPHERES

The governing conduction equation and auxiliary conditions used by Monazam and his coworkers are

$$\rho_1 C_1 \frac{\partial T}{\partial t} = \kappa_1 \frac{1}{r^2} \frac{\partial}{\partial r} \left( r^2 \frac{\partial T}{\partial r} \right), \quad (1)$$

with auxiliary conditions

$$T(r, 0) = T_0, \quad \frac{\partial T}{\partial x}(0, x) = 0, \quad (2)$$

and

$$\kappa_1 \frac{\partial T}{\partial r}(a, t) = \frac{1}{2} \alpha_r I_{\text{inc}}(t) - \left\{ h_c [T(a, t) - T(\infty, t)] + \sigma \epsilon_r [T^4(a, t) - T^4(\infty, t)] \right\} \quad (3)$$

The boundary condition at the surface of the sphere includes the time-dependent intensity,  $I_{\text{inc}}(t)$ , of the pulsed incident beam, the convective heat transfer coefficient,  $h_c$ , and the radiative heat loss. The absorptivity,  $\alpha_r$  is assumed to equal the emissivity,  $\epsilon_r$ , of the particle. Here,  $\kappa_1$  is the thermal conductivity of the microparticle, and  $\sigma$  is the Stefan-Boltzmann constant. The incident intensity in the surface boundary condition is divided by two because the laser beam was split to heat the particle from two sides.

Monazam *et al.* solved this system of equations numerically, but for the conditions used in their experiments an approximate analytical solution can be obtained. This is accomplished by writing the linear approximation

$$T^4(a, t) - T_\infty^4 \cong h_r [T(a, t) - T_\infty], \quad (4)$$

in which  $h_r$  is a radiant energy heat transfer coefficient defined by

$$h_r = \left[ T_m^2(a, \infty) + T_\infty^2 \right] [T_m(a, \infty) + T_\infty] \quad (5)$$

and  $T_m(a, \infty)$  is the mean surface temperature at large times, which can be computed by solving an energy balance on the sphere under the assumption that the heat flux averaged over one cycle is zero at large times

The heat transfer coefficient,  $h_c$ , is  $\kappa_2/a$  for a stagnant gas and for low gas Peclet numbers. For the con-

ditions of the METC researchers,  $h_r$  was less than 10% of  $h_c$ , so the linearization should be accurate at later times. The heat loss at early times is overestimated by this approximation because  $h_r$  is overestimated by using the asymptotic mean surface temperature. Thus, it can be anticipated that the analytical solution developed using approximation (4) will underpredict the temperature at small times but should be accurate after some transient period.

The solution of the linearized problem is

$$\frac{T(x, \tau) - T_0}{T_0} = 2\beta(1 - \text{Bi}) \sum_{n=1}^{\infty} \frac{\sin \lambda_n}{(\sin^2 \lambda_n - \text{Bi})} \frac{\sin \lambda_n x}{x} \int_0^\tau f(\tau') \exp[-\lambda_n^2(\tau - \tau')] d\tau', \quad (6)$$

in which  $\beta$ ,  $\text{Bi}$ ,  $x$  and  $\tau$  are dimensionless parameters and variables defined by

$$\beta = a \alpha_r I_{\text{inc}} / 2 \kappa_1 T_0, \quad \text{Bi} = (h_c + h_r) a / \kappa_1, \quad (7)$$

$$x = r / a, \quad \tau = \kappa_1 t / a^2 \rho_1 C_{p1}.$$

Here the subscript 1 refers to the particle and 2 denotes the gas,  $\beta$  is the dimensionless electromagnetic energy flux,  $\text{Bi}$  is a composite Biot number, and  $f(\tau)$  is the normalized laser pulse function, which is unity for the first 3 ms of a pulse and zero for the next 7 ms for the experimental conditions at METC.

The eigenvalues in Eq. (5) satisfy the transcendental equation

$$\tan \lambda_n = \lambda_n / (1 - \text{Bi}). \quad (8)$$

The solution represented by Eq. (6) is compared with the numerical solution of Monazam and Maloney in Figure 1. The physical parameters they used are  $a = 70 \mu\text{m}$ ,  $\alpha_r = \epsilon_r = 0.85$ ,  $I_{\text{inc}} = 4.50 \text{ MW/m}^2$ ,  $\kappa_1 = 1.675 \text{ W/m-K}$ ,  $\kappa_2 = 0.048 \text{ W/m-K}$ ,  $C_1 = 1466 \text{ J/kg-K}$ , and  $\rho_1 = 1050 \text{ kg/m}^3$ . The Biot number corresponding to their conditions is 0.032. The agreement is excellent at later times, and during the transient period when the time-averaged temperature changes, the analytical solution predicts temperatures only slightly lower than the numerical solution.

A more detailed comparison between theory and experiment is shown in Figure 2 for one cycle in the asymptotic region. The agreement is very good, indicating that the best-fit parameters selected by Monazam and Maloney are consistent with their model of uniform surface heating.

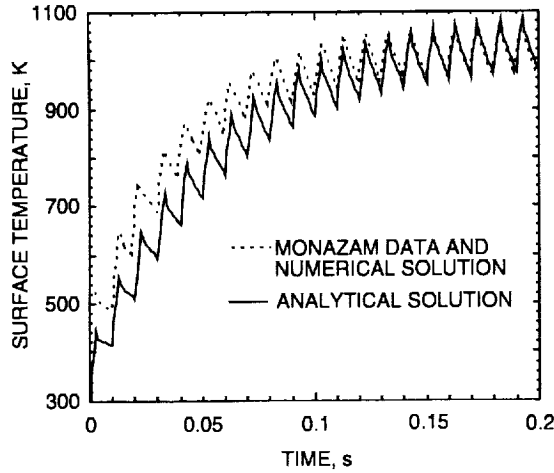


Figure 1. A comparison between theory and experiment for a carbonaceous particle.

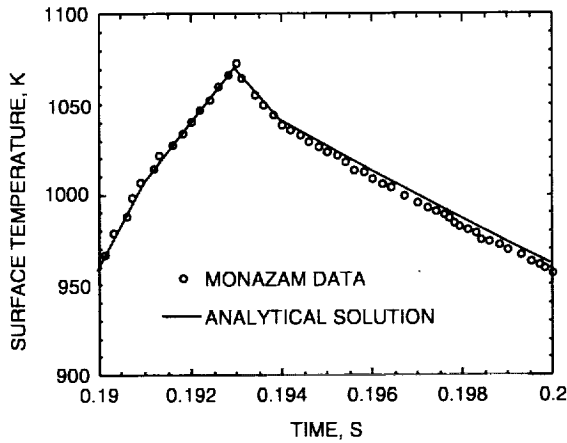


Figure 2. A comparison between theory and experiment for one cycle at later times.

### SPATIALLY NONUNIFORM HEATING

The assumption of uniform surface heating is highly questionable when the thermal conductivity of the particle is not as large as that of carbon. For the 140  $\mu\text{m}$  diameter sphere of Monazam and Maloney, the light scattering size is  $X = 2\pi a/\lambda = 41.498$ . Using a refractive index of  $N = 5.0 + i4.0$ , we computed the source function,  $\mathbf{E}\mathbf{E}^*/E_{\text{inc}}^2$ , presented in Figure 3 for one-sided heating using Mie theory as outlined by Bohren and Huffman [9]. Due to the strong absorption of electromagnetic energy, the source is concentrated near the surface, as assumed by Monazam and Maloney, but the source is highly nonuniform in the  $\theta$ -direction. Our computations indicate that all of the energy absorption is confined to the outer 2% of the sphere, that is, to the region  $x = r/a > 0.98$ , and the

source function is nearly independent of azimuthal angle  $\phi$ .

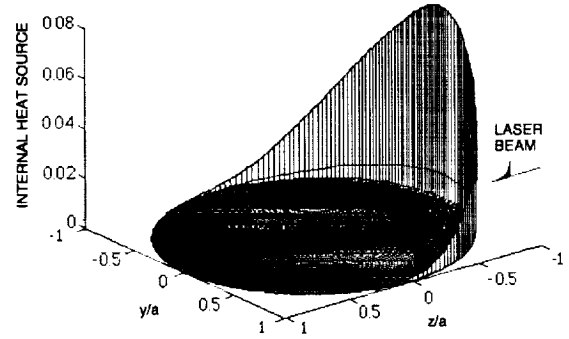


Figure 3. The internal heat source function for a carbonaceous sphere with  $X = 41.498$  and  $N = 5.0 + i4.0$ .

The internal heat generation function for an absorbing sphere is

$$Q(r, \theta, \phi) = \frac{4\pi I_{\text{inc}} \text{Re}[N_1] \text{Im}[N_1]}{\lambda_{\text{inc}}} \frac{\mathbf{E} \cdot \mathbf{E}^*}{E_{\text{inc}}^2}. \quad (9)$$

The pulsed heating problem can now be solved using a source function such as that depicted in Figure 3 or, alternately, as an equivalent surface source problem. For two-sided heating, the shape of the source function, considered as the surface source shown in Figure 3, can be approximated by the intensity distribution

$$I(a, \theta) = I_{\text{max}} \cos^2 \theta. \quad (10)$$

Here  $I_{\text{max}}$  is the intensity at  $\theta = 0^\circ, 180^\circ$ , and  $\theta$  is measured from the direction of propagation of one of the laser beams. This approximation is in very good agreement with the exact surface intensity distribution computed from Mie theory as demonstrated in Figure 4.

When the angular dependence of the temperature distribution is considered, the nondimensional heat conduction equation becomes

$$\frac{\partial U}{\partial \tau} = \frac{1}{x^2} \frac{\partial}{\partial x} \left( x^2 \frac{\partial U}{\partial x} \right) + \frac{1}{x^2} \frac{\partial}{\partial \eta} \left[ (1 - \eta^2) \frac{\partial U}{\partial \eta} \right], \quad (11)$$

in which

$$U = \frac{T - T_0}{T_0}, \quad \text{and} \quad \eta = \cos \theta. \quad (12)$$

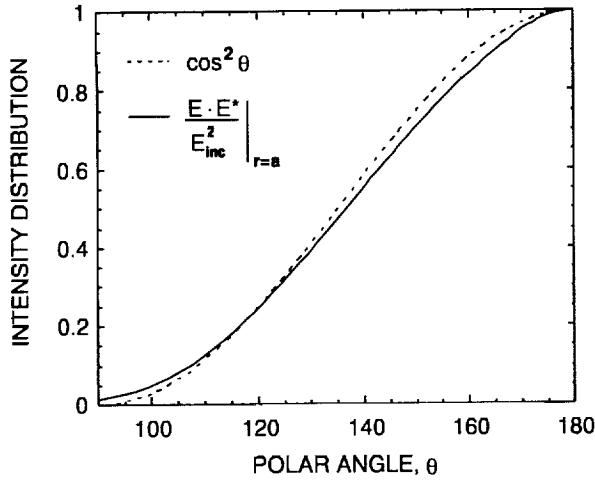


Figure 4. Comparison between the exact solution for the surface intensity distribution and Eq. (10).

The auxiliary conditions are given by

$$U(x, \eta, 0) = \frac{\partial U}{\partial x}(0, \eta, \tau) = 0, \quad (13)$$

and

$$\frac{\partial U}{\partial x}(1, \eta, \tau) = 3\beta f(\tau)\eta^2 - \text{Bi}U(1, \eta, \tau). \quad (14)$$

The solution for the surface temperature is

$$U(1, \eta, \tau) = \frac{\beta}{(2 + \text{Bi})} \{-f(\tau)\} + \sum_{m=1}^{\infty} (6I_1 + \gamma_{m0}^2 I_2) \frac{X_{m0}(1)}{N_{m0}^2} \int_0^{\tau} f(\tau') e^{-\gamma_{m0}^2(\tau-\tau')} d\tau' + (3\eta^2 - 1) \sum_{m=1}^{\infty} \gamma_{m2}^2 I_3 \frac{X_{m2}(1)}{N_{m2}^2} \int_0^{\tau} f(\tau') e^{-\gamma_{m2}^2(\tau-\tau')} d\tau'. \quad (15)$$

Here  $N_{m0}$  and  $N_{m2}$  are the norms of the eigenfunctions  $X_{m0}(x)$  and  $X_{m2}(x)$ , respectively, given by

$$N_{m0} = \sqrt{(\gamma_{m0} - \sin \gamma_{m0} \cos \gamma_{m0}) / \pi \gamma_{m0}^2}, \quad (16)$$

and

$$N_{m2} = \sqrt{\frac{1}{2} [J_{5/2}^2(\gamma_{m2}) + J_{3/2}^2(\gamma_{m2})]} - \frac{5}{2\gamma_{m2}} J_{5/2}(\gamma_{m2}) J_{3/2}(\gamma_{m2}). \quad (17)$$

The eigenfunctions may be written in terms of Bessel functions as

$$X_{m0}(x) = \frac{1}{\sqrt{x}} J_{1/2}(\gamma_{m0}x), \quad (18)$$

and

$$X_{m2}(x) = \frac{1}{\sqrt{x}} J_{5/2}(\gamma_{m2}x). \quad (19)$$

The eigenvalues  $\gamma_{m0}$  satisfy Eq. (8), and the eigenvalues  $\gamma_{m2}$  satisfy

$$\tan \gamma_{m2} = \frac{\gamma_{m2}^3 - 3(3 - \text{Bi})\gamma_{m2}}{(4 - \text{Bi})\gamma_{m2}^2 - 3(3 - \text{Bi})}, \quad (20)$$

The integrals  $I_1$ ,  $I_2$  and  $I_3$  are defined by

$$I_1 = \int_0^1 x^2 X_{m0}(x) dx, \quad (21)$$

$$I_2 = \int_0^1 x^4 X_{m0}(x) dx, \quad (22)$$

and

$$I_3 = \int_0^1 x^4 X_{m2}(x) dx. \quad (23)$$

For Biot numbers larger than those for relatively highly conducting carbon spheres Eq. (15) predicts very large angular variation in the surface temperature. Such variations must be taken into account in the interpretation of data to determine the thermal properties. The surface temperatures at  $\theta = 0^\circ$  and  $90^\circ$  are illustrated in Figure 5 for  $\kappa_1 = 0.167$  W/m-K ( $\text{Bi} = 0.320$ ). The other physical properties are those used by Monazam and Maloney. Additional results have been reported in a paper by Davis and Widmann [12] that is in press.

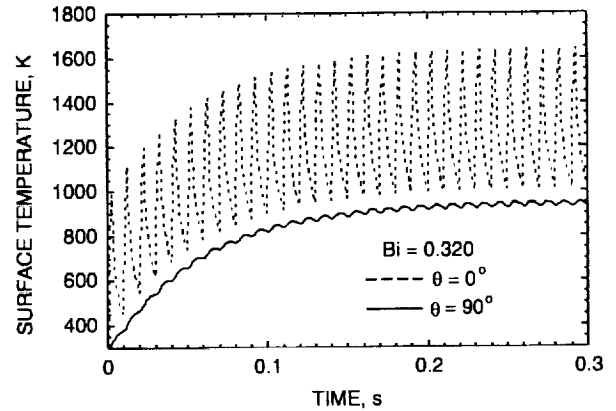


Figure 5. Surface temperature histories for a lower thermal conductivity particle.

## THERMOPHORETIC FORCE

The existing apparatus used for thermophoretic force measurements, which is shown in Figure 6, has been modified to improve the data acquisition system and to facilitate the alignment of the electrodes used for particle levitation. Studies of the effects of natural convection on the thermophoretic force have been carried out over a wide range of system pressures, and Figure 7 shows the levitation voltage as a function of pressure for a polystyrene latex sphere in air.

The change in the levitation voltage (with and without a temperature gradient in the gas phase) yields the ratio of the thermophoretic force to the gravitational force. If  $V_0$  is the dc levitation voltage required to balance the gravitational force,  $mg$ , and  $V$  is the levitation voltage required to balance the particle when gravity and other external forces,  $F$ , act on the particle, the force ratio  $F/mg$  is given by

$$F/mg = (V_0 - V)/V_0. \quad (24)$$

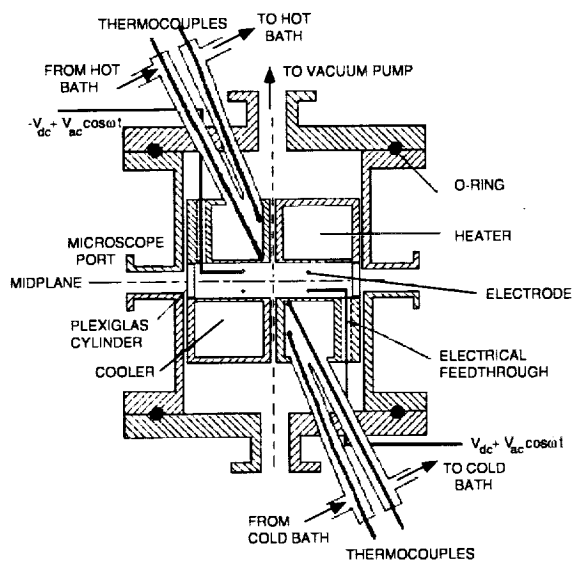


Figure 6. Cross section of the electrodynamic balance used for thermophoretic force measurement.

The external forces can include the phoretic force as well as aerodynamic drag associated with convective motion of the gas.

The data of Figure 7 indicate that for pressures greater than 20 torr natural convection occurred due to edge effects associated with temperature differences between the heat exchangers and the chamber wall, but those effects become negligible as the system pressure decreases. At low pressures the free-molecule regime is reached, and the force becomes independent of pressure.

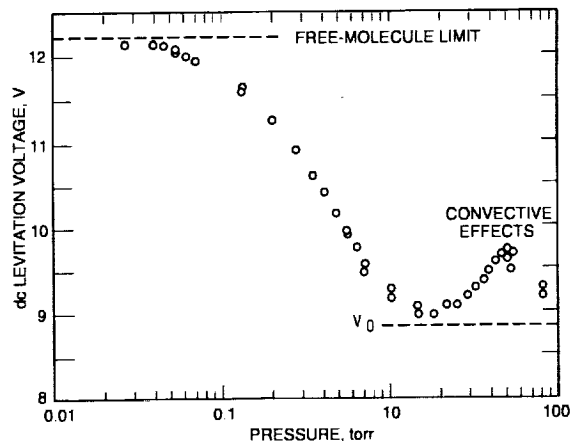


Figure 7. Levitation voltage data for a PSL sphere in air as a function of the chamber pressure.

Data for the intermediate or transition regime (between the continuum regime and the free-molecule regime) are used to determine the accommodation coefficients for momentum and energy transfer between the gas molecules and the microparticle. It is highly desirable to minimize the effects of natural convection, and modifications in the apparatus will be made to do so.

## ACKNOWLEDGMENT

The authors are grateful to NASA for the support of this research through Grant NAG3-1837.

## REFERENCES

1. W. Li and E. J. Davis, Measurement of the Thermophoretic Force by Electrodynamic Levitation: Microspheres in Air, *J. Aerosol Sci.* **26**:1063-1083 (1995).
2. W. Li and E. J. Davis, The Effects of Gas and Particle Properties on Thermophoresis, *J. Aerosol Sci.* **26**:1085-1099 (1995).
3. E. J. Davis, Microchemical Engineering: The Chemistry and Physics of the Microparticle, in *Advances in Chemical Engineering*, Vol. 18, J. L. Anderson, ed., Academic Press, New York, pp. 1-94, 1992.
4. E. J. Davis, A History of Single Aerosol Particle Levitation, *Aerosol Sci. Technol.* **26**, 212-254 (1997).
5. R. E. Spjut, E. Bar-Ziv, A. F. Sarofim and J. P. Longwell, Electrodynamic Thermogravimetric Analyzer, *Rev. Sci. Instrum.* **57**, 1604-1610 (1986).
6. E. Bar-Ziv, D. B. Jones, R. E. Spjut, D. R. Dudek, A. F. Sarofim and J. P. Longwell, Measurement of Combustion Kinetics of a Single Char Particle in an

- Electrodynamic Thermogravimetric Analyzer, *Combust. Flame* **75**, 81-106 (1989).
7. R. E. Spjut, A. F. Sarofim and J. P. Longwell, Laser Heating and Particle Temperature Measurement in an Electrodynamic Balance, *Langmuir* **1**, 355-360 (1985).
  8. E. Bar-Ziv and A. F. Sarofim, The Electrodynamic Chamber: A Tool for Studying High Temperature Kinetics Involving Liquid and Solid Particles, *Prog. Energy Combust. Sci.* **17**, 1-65 (1991).
  9. E. R. Monazam, D. J. Maloney and L. O. Lawson, Measurements of Heat Capacities, Temperatures, and Absorptivities of Single Particles in an Electrodynamic Balance, *Rev. Sci. Instrum.* **60**, 3460-3465 (1989).
  10. E. R. Monazam and D. J. Maloney, Temperature Transients Associated with Pulsed Heating of Single Particles, *J. Appl. Phys.* **71**, 2552-2559 (1992).
  11. C. F. Bohren and D. R. Huffman, *Absorption and Scattering of Light by Small Particles*, John Wiley and Sons, New York, 1983.
  12. E. J. Davis and J. F. Widmann, Pulsed Electromagnetic Heating of Microparticles, *Intl. J. Heat Mass Transfer*, in press (1998).